UNIVERSITY OF BIRMINGHAM
University of Birmingham Research at Birmingham

Geometric neuro-fuzzy transfer learning for in-cylinder pressure modelling of a diesel engine fuelled with raw microalgae oil

Li, Ji; Wu, Dawei; Mohammadsami Attar, Hassan; Xu, Hongming

DOI:
10.1016/j.apenergy.2021.118014

License:
Other (please provide link to licence statement

Document Version
Publisher's PDF, also known as Version of record

Citation for published version (Harvard):
Li, J, Wu, D, Mohammadsami Attar, H & Xu, H 2022, 'Geometric neuro-fuzzy transfer learning for in-cylinder pressure modelling of a diesel engine fuelled with raw microalgae oil', *Applied Energy*, vol. 306, no. Part A, 118014. https://doi.org/10.1016/j.apenergy.2021.118014

Link to publication on Research at Birmingham portal

Publisher Rights Statement:
Contains public sector information licensed under the Open Government Licence v3.0.

https://www.nationalarchives.gov.uk/doc/open-government-licence/version/3/

General rights
Unless a licence is specified above, all rights (including copyright and moral rights) in this document are retained by the authors and/or the copyright holders. The express permission of the copyright holder must be obtained for any use of this material other than for purposes permitted by law.

•Users may freely distribute the URL that is used to identify this publication.
•Users may download and/or print one copy of the publication from the University of Birmingham research portal for the purpose of private study or non-commercial research.
•User may use extracts from the document in line with the concept of 'fair dealing' under the Copyright, Designs and Patents Act 1988 (?)
•Users may not further distribute the material nor use it for the purposes of commercial gain.

Where a licence is displayed above, please note the terms and conditions of the licence govern your use of this document.

When citing, please reference the published version.

Take down policy
While the University of Birmingham exercises care and attention in making items available there are rare occasions when an item has been uploaded in error or has been deemed to be commercially or otherwise sensitive.

If you believe that this is the case for this document, please contact UBIRA@lists.bham.ac.uk providing details and we will remove access to the work immediately and investigate.

Download date: 29. Apr. 2024

Applied Energy 306 (2022) 118014

Contents lists available at ScienceDirect

Applied Energy

journal homepage: www.elsevier.com/locate/apenergy

Geometric neuro-fuzzy transfer learning for in-cylinder pressure modelling of a diesel engine fuelled with raw microalgae oil

Ji Li [a], Dawei Wu [a], Hassan Mohammadsami Attar [b], Hongming Xu [a,*]

[a] Department of Mechanical Engineering, School of Engineering, University of Birmingham, Birmingham B15 2TT, UK
[b] Marine Technology, School of Engineering, Newcastle University, Newcastle upon Tyne NE1 7RU, UK

HIGHLIGHTS

- In-cylinder pressure modelling of a diesel engine fuelled with microalgae oil is carried out.
- A novel approach of geometric neuro-fuzzy transfer learning is proposed.
- Three segmentation patterns are designed for transfer domain of the engine operation region.
- The proposed approach performs superior computational and experimental efficiency.

ARTICLE INFO

Keywords:
Black-box modelling
In-cylinder pressure
Neuro-fuzzy transfer learning
Microalgae oil
Experimental reduction

ABSTRACT

Bioenergy attracts more attention owing to the reduction of both air pollution and greenhouse gas emissions in a whole life cycle compared to fossil fuels. As a third-generation biofuel, Microalgae Oil (MAO) can utilise carbon dioxide and light energy at an increased photosynthetic efficiency compared to energy crops for biomass. Due to the wide variety of MAO and their blends with diesel in different ratios, characterization of these biofuels' engine performance is difficult to be standardized, e.g., in-cylinder pressure. This paper proposes a novel approach of geometric neuro-fuzzy transfer learning (GNFTL) for in-cylinder pressure modelling of a diesel engine fuelled with MAO. Inspired by computational geometry, this approach only utilizes limited experimental data obtained by geometric screening to learn a high-precise transfer model of the in-cylinder pressure with different MAO blending ratios. Followed by the process of MAO extraction and test cell description, the proposed approach of GNFTL is presented which comprises geometric transfer domain segmentation and neuro-fuzzy transfer learning. By a comprehensive study, the results demonstrate that the proposed approach can achieve a competitive prediction accuracy whilst significantly reducing experimental efforts on used biofuel by 47.8% and operation time by 41.5%, compared to the conventional manual design of experiment.

1. Introduction

According to the statistics, internal combustion (IC) engines operating on fossil fuel oil provide about 25% of the world's power, whilst they produce about 10% of the world's greenhouse gas (GHG) emissions [1]. The current share of renewable biofuel production in the overall fuel demand has been found insufficient to replace fossil fuels [2]. Microalgae can deliver a sustainable and complementary biofuel platform with some important advantages, which has lower environmental impact compared to biofuels produced from crops and do not compete with food supply [3]. Among many advantages, the production and use of biofuels from microalgae shows: a high CO_2 sequestration capability [4]; reduction of the use of freshwater [5]; a high concentration of feedstock; value-added coproducts [6]; capability to meet the global demands of energy for transportation [7]. However, strain selection, cultivation method, culture conditions and chemical composition strongly influences biofuel production cost as well as engine's performance and exhaust gas emissions.

In terms of the methodologies applied, the modelling approaches of

Abbreviations: IC, Internal combustion; GHG, Greenhouse gas; MAO, Microalgae Oil; ANN, Artificial neural network; GNFTL, Geometric neuro-fuzzy transfer learning; RSS, Root Sum Square; ANFIS, Adaptive neuro fuzzy inference system; RMSE, Root-mean-squared error; MSE, Mean-square error; St.D., Error standard deviation; DoE, Design of experiment.

* Corresponding author.
E-mail address: h.m.xu@bham.ac.uk (H. Xu).

https://doi.org/10.1016/j.apenergy.2021.118014
Received 23 April 2021; Received in revised form 7 September 2021; Accepted 1 October 2021
Available online 19 October 2021
0306-2619/Crown Copyright © 2021 Published by Elsevier Ltd. All rights reserved.

Nomenclature

p	Power load
n	Engine speed
λ	Blending ratio of MAO
θ	Crank angle degree
RSS	Root Sum Square
εs	System error
εr	Random error
S	Data domain distribution
x	FIS input
F	FIS output
u	Membership degree
c	Fuzzy cluster centre
E	Root-mean-squared error
d	Desired output
y	Model's output
N	The number of data pairs

diesel engines can be categorized as white-box, grey-box, and black-box modelling [8]. As a typical white-box approach, the model of computational fluid dynamics is often used in diesel engine design and performance analysis [9–10]. It is labelled with high accuracy but time-consuming resulting from the calculation of finite element method. The thermodynamic model provides a relatively rapid way to calculate the performance of diesel engine. Its combustion process can be described by multi-zone [11], two-zone [12] and single-zero [13] assumptions. But their accuracy often needs more measured data to help improve (as a grey-box model) [14]. The mean value model regards the work process as a continuous mass and energy flow. The average performance over the engine cycles can be obtained for engine analysis [15], controller design [16], hardware in the loop [17], and fault diagnosis [18]. Owing to the simplification of the in-cylinder process, this model calculates faster than the 0D model, but more measured data is also required to keep the accuracy (as a grey-box model) [19]. In summary, white-box and grey-box modelling approaches could obtain good prediction performance but that relies on expert experience and model accuracy often needs more measured data to help to improve.

Unlike the above two, black-box modelling approaches offer an efficient way to represent a numerical relationship between inputs and outputs under the omission of physical knowledge [20]. Raghuvaran et al. adopt the artificial neural network (ANN) to model performance and exhaust emission on a diesel engine fuelled with different proportions of blends of palm oil biodiesel [21]. The results show great regression behaviour for two input variables of load and blend. Nonetheless, there is a caveat in which proper training of the ANN is essential to avoid the notion of overfitting as well as measurement errors. Hosseini et al. develop a twelve-input and twelve-output ANN for evaluating performance, emission, and vibration of a diesel engine using alumina nano-catalyst added to diesel–biodiesel blends [22]. Multi-task learning can be efficiently handled by a multilayer perceptron network, but a large number of input variables make it difficult to apply in practice. Adaptive neuro-fuzzy inference system also has been widely applied for performance prediction and optimization of diesel engines fuelled with biofuel, such as diesel-palm oil [23], diesel-algal oil [24], and diesel-Kusum [25]. Besides, optimization algorithms such as Genetic Algorithm [26] and Particle Swarm Optimization [27] can be used that enable gradient-free agent to further optimize ANN-driven prediction model of engine performance. Response surface methodology as one of typical analytical approaches is often adopted for engine performance modelling. Its prediction performance is competitive for predicting some performance indicators e.g., emissions [28] and output power [29]. However, such existing black-box modelling approaches for diesel engines require a large amount of experimental dataset, which undoubtedly will be time-consuming and expensive (for material and operation cost) for the development of diesel engines fuelled with new biofuels.

Currently, governments worldwide have adopted and enforced

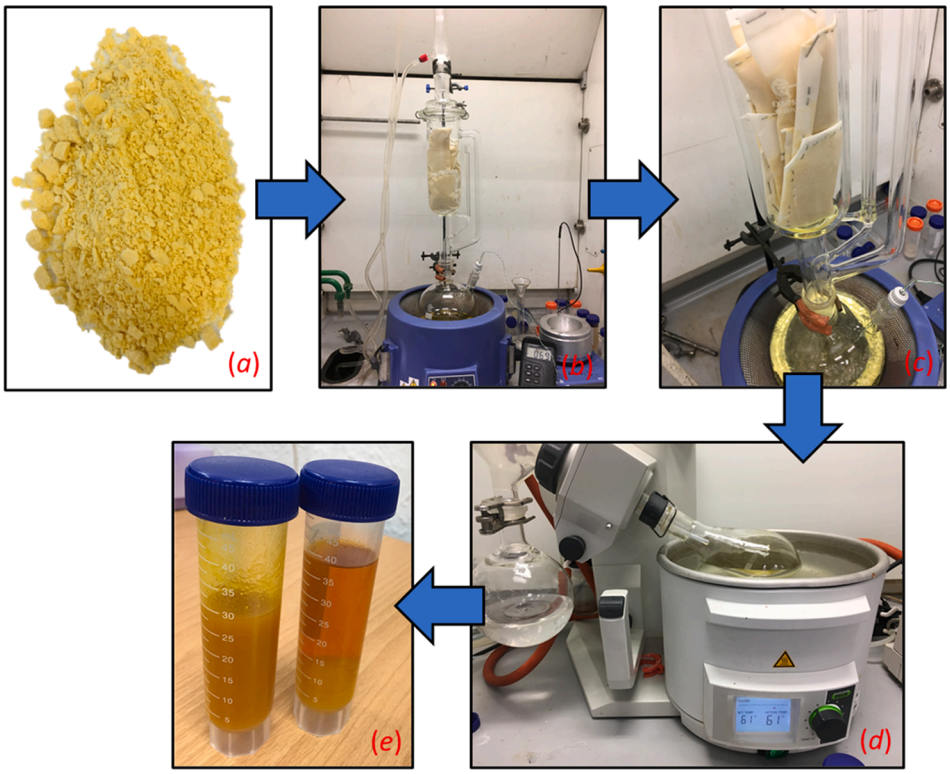

Fig. 1. Soxhlet extraction method: (a) Dried microalgae biomass (b) Soxhlet extractor (c) Mixture of Hexane and MAO (d) Rotary evaporator (e) Extracted MAO.

Table 1
Properties of the Schizochytrium sp. Raw MAO and diesel oil.

Properties	Diesel oil	MAO	Unit
Kinematic viscosity at 50°C	1.811	19.67	cSt
Density	762.5	930	kg/m^3
Calorific value	42.8	36.84	MJ/kg
Carbon	86	75.9	%
Hydrogen	14	10	%
Oxygen	0	14	%
Flashpoint	52	180	°C

stricter-than-ever emission legislation to prevent the deterioration of the environment [30]. It makes the calibration of vehicle engines fuelled with such new biofuel more challenging in terms of balancing the need for dynamics, emissions, and economy [31]. Using the in-cylinder pressure as an indication, engine calibration becomes easier because most of the required information for engine controls can be derived from the in-cylinder pressure such as brake thermal efficiency [32]. In light of this, an accurate, fast-response, and low-development-cost prediction model of in-cylinder pressure is essential in the optimization of diesel engines fuelled with new biofuels.

Rapid development in informatics enables fast and cheap modelling of complex physical systems based on the measurement of real-world performance [33–34]. Because of avoiding much expensive data-labelling efforts, transfer learning has been emerging as a new learning framework to improve the performance of learning [35]. In the development of a diesel engine fuelled with a new biofuel, biofuel preparation and experimental operation are always expensive and time-consuming. Raw MAO is one of the promising biofuels to achieve decarbonisation, where its combustion behaviour is largely affected by the blending ratio found in our recent research [36]. To reduce experimental efforts and ensure prediction accuracy, this paper, for the first time, proposes a novel approach of geometric neuro-fuzzy transfer learning (GNFTL) for in-cylinder pressure modelling of a diesel engine fuelled with MAO. Inspired by computational geometry, this approach only utilizes limited experimental data obtained by geometric screening to learn a high-precise transfer model of the in-cylinder pressure with different MAO-diesel blends. Differing from the conventional data-driven modelling approaches, the proposed GNFTL approach is used to pre-define transfer domains before initializing and tuning hyper-parameters of the ANFIS for saving computational and experimental costs. The experimental dataset is obtained from steady-state tests carried out in a Lombardini 15 LD 225 diesel engine fuelled with MAO. For this model to be valid, we assume the dataset obtained includes boundary values of the studied engine in study. An extensive numerical study of the proposed approach is carried out for comparison of the-state-of-the-art approaches.

2. Experimental Set-up

2.1. Microalgae oil extraction

To effectively extract the MAO from Schizochytrium sp. biomass, the commonly used Soxhlet extraction (chemical) method [37] is adopted. In the process of Soxhlet extraction, firstly, the microalgae biomass in Fig. 1(a) is placed inside a thimble filter paper. Secondly, as shown in Fig. 1(b), the thimbles are placed into the main chamber of the Soxhlet extraction equipment. Thirdly, the extraction solvent (Hexane) is placed in a distillation flask. It is clear from Fig. 1(c) that MAO was successfully extracted from the biomass. For separating the solvent from the extracted oil, the mixture in Fig. 1(d) is placed in a rotary evaporator. Using a rotary evaporator in the extraction process will separate the oil from the hexane and will also recover the hexane for future use.

In order to alleviate any injection and combustion difficulties in the diesel engine, a preheating process should be carried out to reduce the viscosity of the microalgae oil. In this study, the engine fuel system has two additional heating processes to maintain the biofuel temperature between 55 and 65 degreesC. The properties of the MAO and diesel oil are illustrated below in Table 1. Because Microalgae oil has poor fluidity below 50 degrees and usually cannot be directly mixed with diesel, for a fair comparison, the Kinematic viscosity of these two types of oils at 50 degrees is presented here.

Table 2
Engine specification.

Parameter	Value	Parameter	Value
Num. of cylinders	1	Max. speed	3600 rpm
Cycle	4-stroke	Max. torque	10.4 Nm at 2400 rpm
Power	3.5 kw	Injection system	Direct
Bore	60 mm	Aspiration	Natural
Compression ratio	21:1	Cooling system	Air

2.2. Test cell description

The experiment test bench P8250 consists of a Lombardini 15 LD 225 diesel engine, which is established by Cussons Technology Ltd. The engine specification is summarised in Table2. For enabling the use of biofuel, this test bench, as illustrated in Fig. 2, has been slightly modified by adding some critical sensors, data acquisition, and a new fuel system with a preheating unit. A 3-phase Prestolite 66,021,637 electrical alternator is connected to the engine via toothed pulleys and a toothed belt. Additionally, the alternator is fitted with a 3-phase bridge reaction circuit. The electric output power from the alternator is dissipated in a controllable electric heater, as a load bank mounted within the test bench frame. The front panel has a fuel flow measuring burette connected to the fuel line via a two-way valve to allow fuel to be drawn from the burette when it switched to the measuring position. Another three-way valve is connected to the fuel line before the measuring valve and is used to switch between diesel oil and MAO tanks. At the intake side, a plenum chamber is also mounted on the test bench to measure the airflow by using a differential pressure transducer that is displayed in a digital form through a digital meter in the front panel. A resistance type load bank is mounted on the rear of the front panel in order to dissipate the rectified DC output from the alternator. An electric fan cools the load bank to prevent a build-up of any potential heat. There is a rotary knob on the side of the control panel that is used to control the load applied to the engine. The output voltage and current are displayed via an analogue voltmeter and ammeter. Temperature sensors were added to the test bench in order to monitor the critical temperatures during the experimental work, e.g., the MAO temperature inside the tank and before injection, cylinder head and lubricant oil temperatures.

2.3. Experimental data and error analysis

Collection process of experimental data has three main steps: 1) engine warm-up 2) testing and sampling; and 3) oil change, wherein Step 2 and 3 will be carried out alternately during the testing process. The testing time (for each scenario) and oil change time are both 30 mins in average. After stable engine operational condition achieved (cyclic variation $\leq$ 5%), the first 5 cycles of in-cylinder pressure data while the engine performs with minimum errors of power load and speed against set values are selected as contending candidates. Based on the five contending candidates, the mean-value cycle is calculated and regarded as a target cycle. The representative cycle is sorted out from the contending candidates which has the lowest integral time absolute error compared to the target cycle.

There are many variables considered in empirical modelling of in-cylinder pressure [24,32,38–39], such as crank angle, ignition timing, engine speed, power load, blending ratio, duct pressure, temperature,

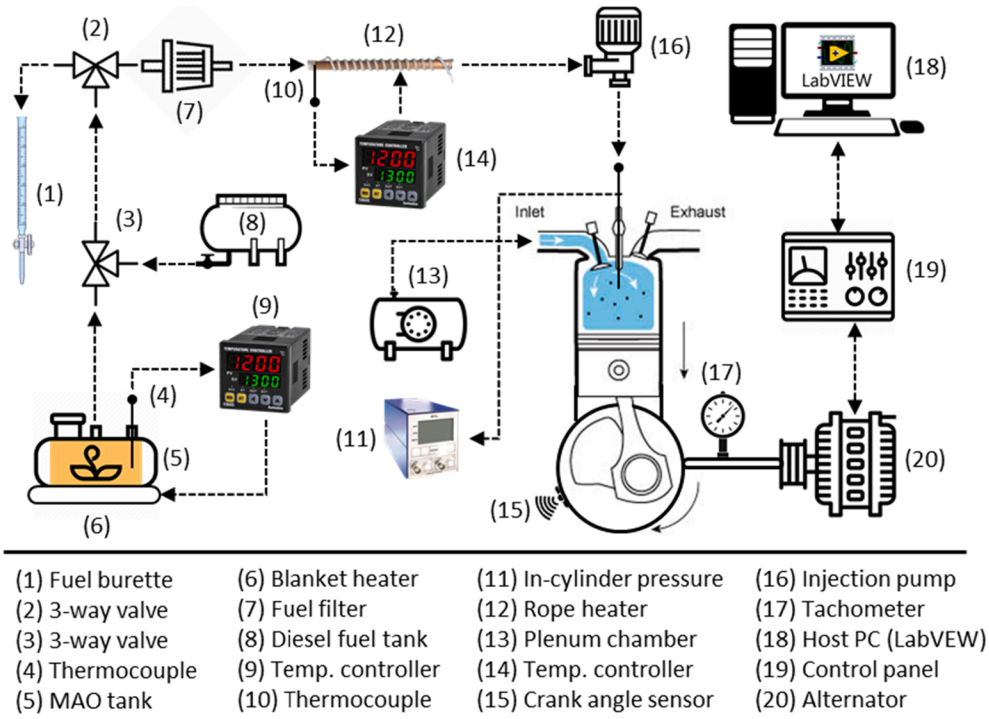

Fig. 2. Schematic diagram of the engine test bench.

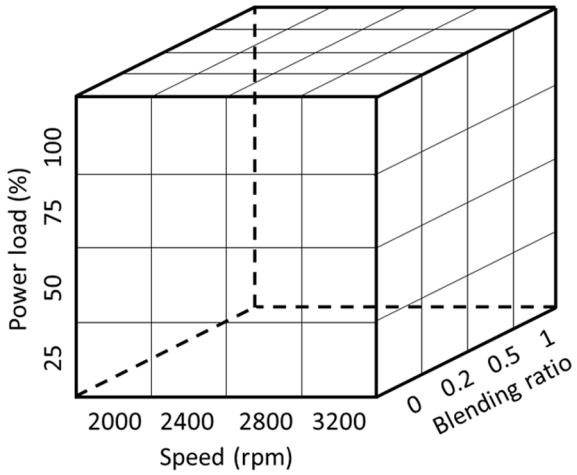

Fig. 3. Experimental data distribution.

and ion current signals. For this study, multi-input-one-output model structure is adopted as expressed in Eq. (1). Input variables include power load (%), $p = [25, 50, 75, 100]$; engine speed (rpm), $n = [2000, 2400, 2800, 3200]$; blending ratio of MAO, $\lambda = [0, 0.2, 0.5, 1]$; and crank angle degree (°), $\theta \in [-100, 100]$. The output is in-cylinder pressure (bar), *Pressure*.

$$Pressure = f(p, n, \lambda, \theta) \tag{1}$$

In order to facilitate the analysis of experimental data, data visualization is carried out based on three discrete input variables i.e., power load, rotational speed, and blending ratio. As displayed in Fig. 3, each of the three discrete input variables has four levels. Each small cube comprises time-series measured data of crank angle degree and in-cylinder pressure at a specific condition of power load, rotational speed, and blending ratio.

Errors in experimental studies and the resultant measurements occur and include both random and systematic errors. The sources of these errors are wide ranging and include experimental planning, instrument selection, condition of the instrument, calibration, environmental conditions, observation of measurement, and measurement reading. Therefore, to demonstrate the accuracy of experimental studies, uncertainty analysis can be utilised. The random error refers to an accidental and unanticipated change in the experimental conditions, for example, mechanical variation, electrical interference, sensor or temperature variation. The systematic error is non-random and is determined as the difference between the actual value and the mean value. In this project, the experimental error and uncertainty were calculated by using the statistical tolerance analysis method Root Sum Square (RSS), using the following equation:

Table 3
Data measurement error.

Parameters	Uncertainties
Engine speed	±10rpm
Brake power	±2.5%
Fuel consumption	±3%
In-cylinder pressure	±2%

$$RSS = \sqrt{(\varepsilon s)^2 + (2\varepsilon r)^2} \tag{2}$$

where εs is a system error, and εr is a random error. The relative percentage uncertainties of various parameters are calculated, as shown in Table 3.

3. Geometric Neuro-Fuzzy transfer learning

To reduce experimental efforts and ensure prediction accuracy, this paper proposes a novel approach of geometric neuro-fuzzy transfer learning (GNFTL) for in-cylinder pressure modelling of a diesel engine fuelled with MAO. This approach consists of two main procedures: 1) geometric transfer domain segmentation and 2) neuro-fuzzy transfer learning. Firstly, three segmentation schemes of geometric transfer

domain will be designed to determine the dataset for source and target domains. Secondly, adaptive neuro fuzzy inference system (ANFIS) model will be developed and used as transfer learning structure. Different methods of fuzzy space partition will be applied to generate the fuzzy rules and MF scalar parameters for in-cylinder pressure model by using the data from source domain. Finally, all parameters will be re-calibrated by using the additional data from target domain.

3.1. Geometric transfer domain segmentation

To reduce experimental effort (i.e., fuel consumption and operation time), the demand of much expensive labelled data for both source domain and target domain needs to be greatly reduced. Considering the particularity of the cylinder pressure experiment, the smallest unit of the experimental workload is for one specific working condition (as shown as one small cube in Fig. 3), rather than the traditional way to reduce random samples. If reducing the labelled sample in this way, however, this will cause the labelled sample to not cover the entire operation region of the engine.

In the light of this, a design scheme of geometric transfer domain segmentation is proposed to formulate this situation as a multi-task transfer learning problem [35] and try to minimize feature loss weakens during learning the target and source task simultaneously. Three segmentation patterns are designed to allocate source and target domains in the engine operation region as displayed in Fig. 4, wherein the source domain data is marked in purple and target domain data is marked in green.

Three source domains assigned by the segmentation patterns are all fixed at eight cubes with three-dimension (3D) boundary in the engine operation region. The three target domains are set to be flexible for assignment. According to the attribute of boundary data, they can be defined as 1D (Fig. 4(a)), 2D (Fig. 4(b)), and boundary-interior mixed (Fig. 4(c)) segmentations. Here, the data domain distribution S of using geometric transfer domain segmentation can be alternatively represented as follows:

$$S_a = \left[S_{a,1}S_{a,2}S_{a,3}S_{a,4}\right] = \begin{bmatrix} 1&0&0&1 & 0&2&2&0 & 0&2&2&0 & 1&0&0&1 \\ 0&2&2&0 & 2&0&0&2 & 2&0&0&2 & 0&2&2&0 \\ 0&2&2&0 & 2&0&0&2 & 2&0&0&2 & 0&2&2&0 \\ 1&0&0&1 & 0&2&2&0 & 0&2&2&0 & 1&0&0&1 \end{bmatrix} \tag{3}$$

$$S_b = \left[S_{b,1}S_{b,2}S_{b,3}S_{b,4}\right] = \begin{bmatrix} 1&2&2&1 & 2&0&0&2 & 2&0&0&2 & 1&2&2&1 \\ 2&0&0&2 & 0&0&0&0 & 0&0&0&0 & 2&0&0&2 \\ 2&0&0&2 & 0&0&0&0 & 0&0&0&0 & 2&0&0&2 \\ 1&2&2&1 & 2&0&0&2 & 2&0&0&2 & 1&2&2&1 \end{bmatrix} \tag{4}$$

$$S_c = \left[S_{c,1}S_{c,2}S_{c,3}S_{c,4}\right] = \begin{bmatrix} 1&0&0&1 & 0&0&0&0 & 1&0&2&2 & 1&0&2&1 \\ 0&0&0&0 & 0&2&2&0 & 0&2&2&2 & 0&2&2&2 \\ 2&2&0&0 & 2&2&2&0 & 0&2&2&0 & 0&2&2&0 \\ 1&2&0&1 & 2&2&0&0 & 0&0&0&0 & 1&0&0&1 \end{bmatrix} \tag{5}$$

where, '0′ indicates unsupervised domain (non-labelled) data; '1′ indicates source domain data; '2′ indicates target domain data. The detail of the three typical designs is organized as Table 4. Data volume including three types of different domains i.e., source, target and unsupervised domains will be used in the next section for the hyperparameters' initialization, hyperparameters' re-tuning, and validation, respectively. It should be noted that there is a small variation in the sampling volume under each specific working condition, but all include the complete cycle of in-cylinder pressure.

Here, Spearman's rank correlation coefficient is used to perform sensitivity analysis of data from different transfer domains. As illustrated in Fig. 5, crank angle degree has the strongest positive correlation to in-cylinder pressure, compared to the other 3 features. From a view of transfer domains, data from the source domain has the lowest correlation to in-cylinder pressure. The authors think the reason behind this is that the data of 8 vertices are quite different. Besides, the correlation of three target domains to in-cylinder pressure all has a certain improvement.

3.2. Neuro-Fuzzy transfer learning

Based on the transferability of neural networks, network-based transfer learning is incorporated with fuzzy rules i.e., neuro-fuzzy transfer learning to realize the model expansion of in-cylinder pressure prediction to the source, target, and unsupervised domains. The basic principle is to reuse the partial neuro-fuzzy network that has been pre-trained in the source domain and utilize it to initialize the specific parts of the neuro-fuzzy network in the target domain, as shown in Fig. 6. The key idea of such a treatment is to transform data into internal representations, in which generic features extracted by neuro-fuzzy networks can be reused in similar domains [40]. In the context of transfer learning, it targets to optimize the spaces of weights and bias by hybrid algorithm, which incorporates the least square estimation to the backpropagation method to accelerate the convergence, and the parameters of neural networks are the internal representations of data.

Generally, the implementation of the neuro-fuzzy transfer learning can be divided into four steps: the first step is to determine the ANFIS structure based on $Pressure = f(p, n, \lambda, \theta)$. The second step is to classify fuzzy space for representations of a number of input–output pairs in the source domain until the fuzzy C-mean clustering algorithm converges to a stable and desired state. Afterwards, internal representations of the source domain excluding rules are utilized to initialize the same neuro-fuzzy network parameters of both source and target domains while constantly fixing the network structure. Ultimately, data of the unsupervised domain will be considered to verify the migration performance of in-cylinder pressure prediction.

3.3. ANFIS structure determination

ANFIS is an artificial intelligence way used for solving complicated and extremely nonlinear issues [41]. As ANFIS integrates with both FIS and ANN, it is effective at solving nonlinear and complex problems in one framework. The ANFIS structure used in this study contains four inputs plus five layers. In this structure, the Takagi-Sugeno fuzzy system was employed as FIS. To explain the process of ANFIS, it was considered that the FIS contains two inputs (x_1, x_2) and one output (F). Typically,

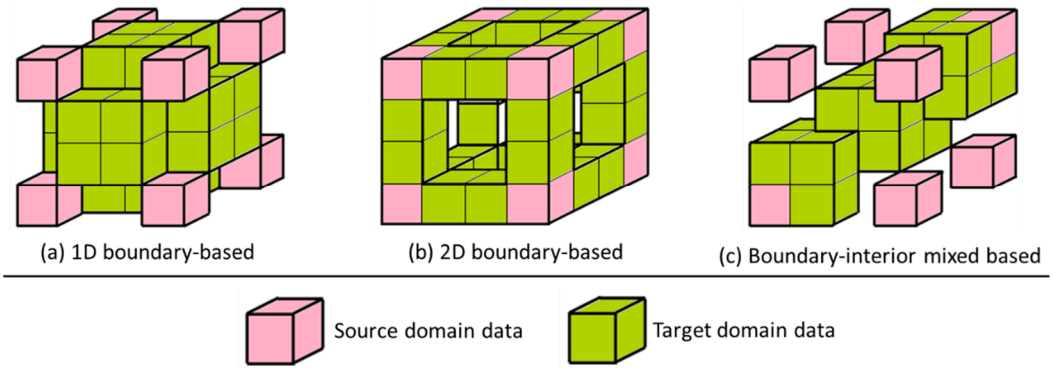

Fig. 4. Three designed segmentation patterns for transfer domain of the engine operation region.

the fuzzy rules can be reported in the following way [42]:

$$\text{Rule1}: \text{If} x_1 \text{is} I_1 \text{and} x_2 \text{is} J_1 \text{and etc.}; \text{then} F_1 = a_1x_1 + b_1x_2 + \cdots + r_1;$$

$$\text{Rule2}: \text{If} x_1 \text{is} I_2 \text{and} x_2 \text{is} J_2 \text{and etc.}; \text{then} F_2 = a_2x_1 + b_2x_2 + \cdots + r_2;$$

where x_1 and x_2 are the inputs. $a_1; b_1; r_1; a_2; b_2; r_2$ are the output's (O) function parameters. I_1, I_2, J_1, J_2 are the membership functions for inputs (x_1 and x_2). The fundamental configuration of ANFIS is feed-forward network that contains five layers with various functions. The function of each layer is presented in Eqs. (6)–(11). With input nodes in layer 1, the membership relationship involving the input and output functions of this layer is referred to as:

$$F_{1,i} = \mu_{Ai}(I), i = 1, 2 \tag{6}$$

$$F_{1,i} = \mu_{Bi}(J), i = 1, 2 \tag{7}$$

In rule nodes or layer 2, this layer's output is the input signal's product that is referred to as

$$F_{2,i} = W_i = \mu_i(I)\mu_i(J), i = 1, 2 \tag{8}$$

where $\mu_i(I)$ and $\mu_i(J)$ are the membership functions. In normalized layer or layer 3, the weight function is under normalization as:

$$F_{3,i} = w = \frac{w_i}{w_1 + w_2}, i = 1, 2 \tag{9}$$

In consequent nodes or layer 4, which is defuzzied layer, the output from the prior layer is multiplied with the Sugeno fuzzy rule's function:

$$F_{4,i} = \overline{w}_i f_i = w_i(a_1x_1 + b_1x_2 + \cdots + r_1), i = 1, 2 \tag{10}$$

In output node with one node (layer 5), the sum of all outputs of every rule from the last layer is calculated.

$$F_{5,i} = \sum_{i=1}^{n} \overline{w}_i f_i = \frac{\sum_{i=1} w_i f_i}{\sum_{i=1} w_i} \tag{11}$$

3.4. Fuzzy space partition

Fuzzy space partition plays a decisive role in the ANFIS on determining the fuzzy space of Takagi-Sugeno fuzzy system and outcome of the if-then rules. Conventionally, the fuzzy space is partitioned by grid partition or subtractive clustering, which are simple or crude hard clustering methods and cannot effectively fulfil fuzzy space partition. In our study, fuzzy C-mean clustering algorithm is introduced to learn knowledge of the source domain, which is mainly based on the fuzzy logic in which the discussion of the membership function and the membership of a sample is presented in several clusters. By assuming that the data set is X and dividing X into C fuzzy clusters, the objective function J is obtained in an environment where the fuzzy coefficient is m:

$$J = \sum_{i=1}^{N} \sum_{j=1}^{C} u_{ij}^{m} \|x_i - c_j\|^2, 1 \le m \le \infty \tag{12}$$

where u_{ij} represents the membership degree of the ith sample to the centre of jth fuzzy cluster contrary to each sample only belongs to one group, and c_j represents the jth fuzzy cluster centre:

$$u_{ij} = \frac{1}{\sum_{k=1}^{C} \frac{\left(\|x_i - c_j\|\right)^{\frac{2}{m-1}}}{\|x_i - c_k\|}} \tag{13}$$

$$c_j = \frac{\sum_{i=1}^{N} u_{ij}^{m} \bullet x_i}{\sum_{i=1}^{N} u_{ij}^{m}} \tag{14}$$

Once fuzzy C-mean clustering algorithm converges to a stable and desired state, the fuzzy rules will be fixed, and its neuro-fuzzy network parameters will pass to the next step as the initial condition.

3.5. Transfer learning for tuning parameters

For achieving high performance in a complete range of in-cylinder pressure prediction, multi-task transfer learning is developed to learn the target and source task simultaneously. The advantage of this treatment is to avoid the overfitting by the source domain data (original 8 vertex data) and describe the non-linearity of all data by transferring knowledge from both source and target domain data. In order to implement knowledge transfer, the ANFIS uses a two-pass learning algorithm to re-tune the neuro-fuzzy network parameters, i.e., forward pass and backward pass. In the forward pass, the premise parameters are not modified, and the consequent parameters are computed using the least squares estimate learning algorithm. In the backward pass, the consequent parameters are not modified, and the premise parameters are computed using the gradient descent algorithm. Based on these two learning algorithms, ANFIS adapts the parameters in the adaptive network. Commonly, a learning algorithm owns a single objective (approximation error minimization) that is often achieved by minimizing the root-mean-squared error (RMSE) on the learning data.

Table 4
Detail of three segmentation pattern designs for transfer domain.

Segmentation pattern	Ratio of known regions	Data volume		
		Source domain	Target domain	Unsupervised domain
1-D	(8 + 24)/64	788	2610	4781
2-D	(8 + 24)/64	788	2960	4431
Mixed	(8 + 22)/64	788	1888	5503

Note: Ratio of known regions = (source domain data + target domain data)/ entire data

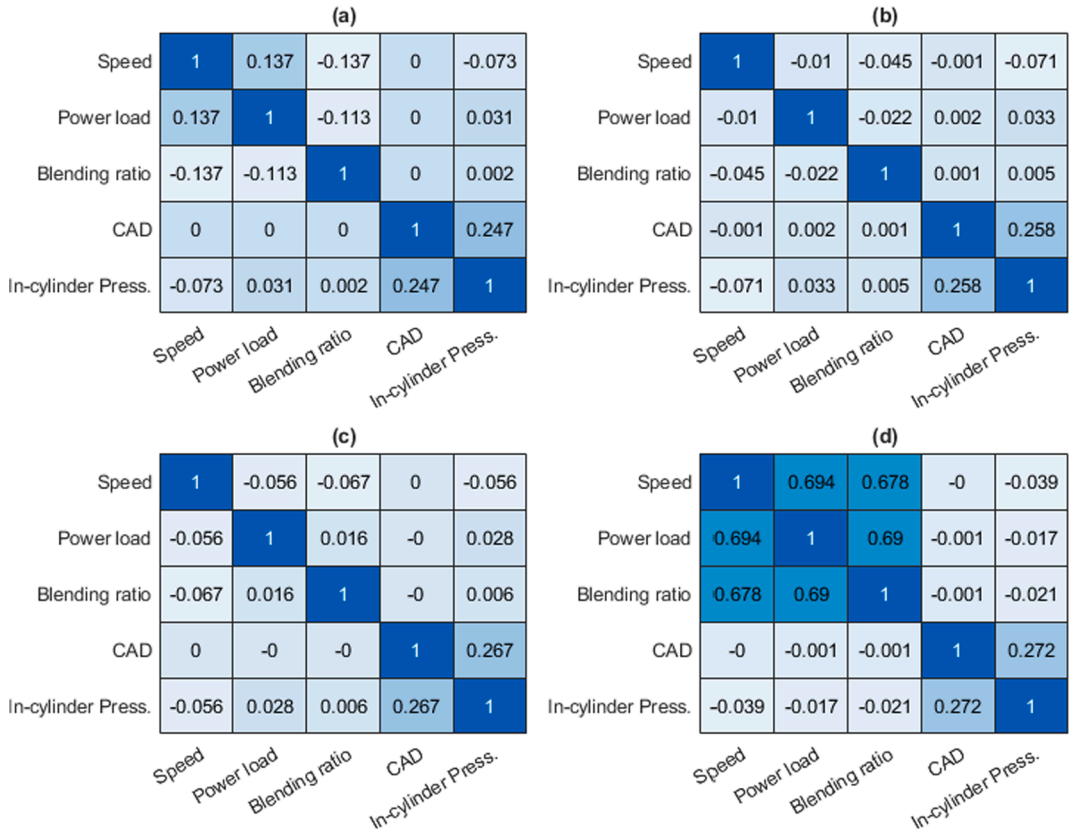

Fig. 5. Spearman's rank correlation coefficient comparison of: a) source domain; b) 1-D target domain; c) 2-D target domain; and d) mixed target domain.

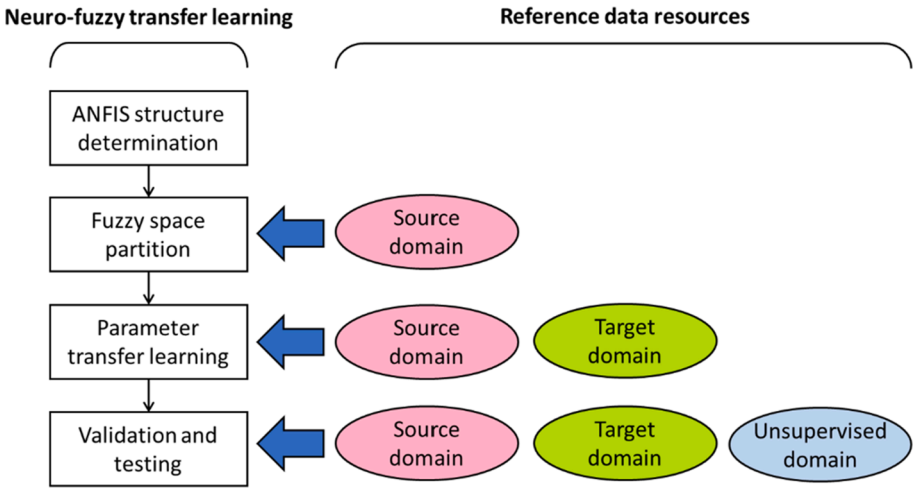

Fig. 6. Workflow of neuro-fuzzy transfer learning.

$$E = \sqrt{\frac{1}{N}\sum_{i=1}^{N}(d_i - y_i)^2} \tag{15}$$

where d and y are the desired and the model's outputs, respectively, and N is the number of data pairs in the training set. In this paper, the selection of the best phenotype in a single objective training was solely based on a comparison of the RMSEs. Once terminal condition reached, iterations will be ended. The final hyperparameters of ANFIS will be fixed for function validation and testing of entire data from source, target, and unsupervised domains.

4. Results and discussion

From here on, a comprehensive comparative study for the proposed GNFTL is carried out from four aspects of 1) impact of segmentation patterns; 2) transfer learning vs. non-transfer learning; 3) comparison of fuzzy space partition methods; and 4) contribution on experimental reduction.

4.1. Impact of segmentation patterns

This section investigates the impact of three designed segmentation patterns for transfer domain of the engine operation region on in-

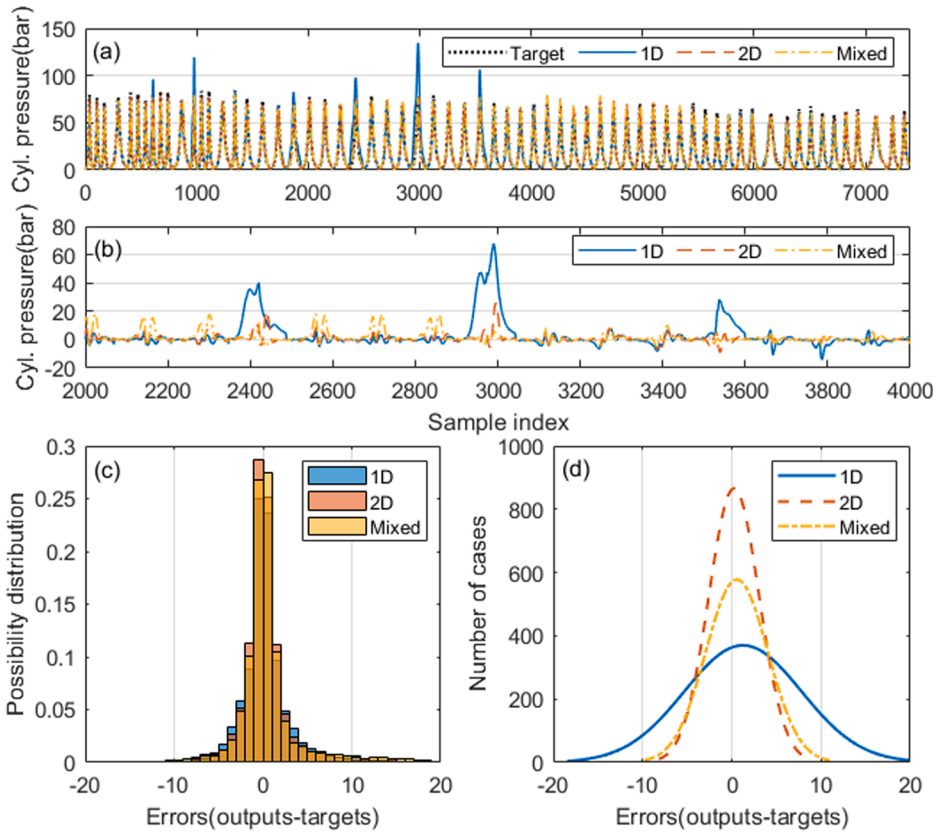

Fig. 7. Performance of using three designed segmentation patterns: a) prediction performance comparison; b) error comparison; c) possibility distribution of errors; and d) normal density function fitting.

cylinder pressure modelling. They are 1D boundary, 2D boundary, and boundary-interior mixed segmentations. Dataset split ratio of training and testing for each domain is set to 70/30 and the repeatability experiment is carried out 20 times.

Fig. 7 shows the best performance of using three designed segmentation patterns obtained from the repeatability experiment. From Fig. 7 (a), the prediction performance of using 2D and mixed segmentation patterns both are more precise and stable than that of using 1D segmentation pattern. Through further observation of sample index [2000,4000] as shown in Fig. 7(b), three peaks caused by 1D segmentation can be found and their sample indexes are 2400 (rpm@2400/blending ratio@1/power load@0.5), 3000 (rpm@2400/blending ratio@1/power load@0.75), 3550 (rpm@2400/blending ratio@1/power load@1), respectively. The authors think the reason behind is the in-cylinder pressure has a strong nonlinearity on the specific condition with rpm@2400 and blending ratio@1. Since the mixed segmentation ignores the target domains on both sides of the cube diagonal, function approximation will be proceeded to directions of the diagonal and eight vertices, so that the error will be relatively evenly apportioned to the unsupervised domain. From Fig. 7(c)(d), basically, the errors are concentrated in the interval $[-5,5]$, in which the distribution of using 2D segmentation pattern is narrower than the other two.

Table 5 summarises four evaluation metrics of three designed segmentation patterns. It is worth mentioning that 2D segmentation has scored first in all four metrics of mean-square error (MSE), RMSE, error mean, and error standard deviation (St.D.) Compared to 1D and mixed segmentations, 2D segmentation can significantly reduce the RMSE of 57.5% and 19.3%, respectively. Error St.D. can be also reduced by 41.7% and 18.4%, respectively. Such evidence demonstrates that the prediction model of using 2D boundary segmentation has stronger robustness and this pattern will be adopted for the following discussion.

4.2. *Transfer learning vs Non-transfer learning*

This section evaluates the prediction performance of using transfer learning and non-transfer learning, in which the terminal conditions for both transfer learning and non-transfer learning are maximum iteration number, $T = 200$, for a fair comparison. Different from transfer learning, non-transfer learning always uses data from both source and target domain to train the ANFIS model. For quantitative analysis of benefits of transfer learning, several metrics as defined in [43] such as jumpstart (before learning), asymptotic Performance, Total Reward, Transfer Ratio, and Time to Threshold are generally considered. In conjunction with our specific studied case, the evaluation metrics for transfer learning of in-cylinder pressure modelling are redefined as: 1) prediction accuracy (validation data), ΔP; 2) jumpstart (before learning), ΔJ; 3) time to converge, ΔT; and 4) generalization performance (testing data), ΔG.

Fig. 8 shows real-time performance comparison of non-transfer and transfer learning, wherein training, validation, and testing data are simultaneously observed in both iteration process of non-transfer and transfer learning. Thanks to the pretrain of the ANFIS model by using source domain data, as illustrated in Fig. 8(a), using transfer learning can effectively reduce initial error (before learning) by $\Delta J = 4.057(-59.0\%)$ and time to converge by $\Delta T = 76(-50.7\%)$, compared to using non-transfer learning. In the observation of validation data as Fig. 8(b) shown, although the gap of time to converge between non-transfer and transfer learning has a certain degree of reduction, the prediction accuracy of using transfer learning is still much higher than that of using non-transfer learning, $\Delta P = 3.44(-64.0\%)$.

Fig. 8(c) expresses the observation of testing data which can be seen that RMSE of the ANFIS model using non-transfer learning is significantly much higher than that of using transfer learning, $\Delta G = 3671.7(-99.9\%)$. Through analysis of the four metrics, the transfer learning for in-cylinder pressure modelling has absolute advantages contrast to traditional non-transfer learning. The reasons for such a large gap will be discussed in the follow-up.

Fig. 9 and Fig. 10 display the regression performance of using non-transfer and transfer learning, respectively. From Fig. 9(d), using traditional non-transfer learning can lead to severe overfitting. This may be due to excessive belief in the source and target domains, and these two domains are only partial representations of the whole domain including unsupervised domain. Relatively, using transfer learning firstly uses eight vertex data (source domain) to pre-train and locate the hyperparameters of ANFIS model. Such a treatment is a restriction on the moving range of these hyperparameters in the second training and to differentiate the characteristics of the source domain and the target domain for avoiding the assimilation of the two. As results from Fig. 10, it shows excellent regression performance of transfer learning especially in the aspect of generalization performance (testing data).

4.3. Comparison of fuzzy space partition methods

After verifying the advantages of GNFTL, this section will further investigate a suitable fuzzy space partition method applied in ANFIS model with most computationally efficient. One computer equipped with i7-10750H @ 2.60 GHz is deployed for all tasks. There are three fuzzy space partition methods of grid partition, subtractive (sub.) clustering, and fuzzy C-mean. According to their own partition techniques, the studied ranges for their three is described as follows:

1) Grid partition - rules of each MF: $[2^4\ 3^4\ 4^4]$
2) Sub Clustering - influence radius: [0.3 0.4 0.5 0.6 0.7 0.8 0.9 1.0]
3) Fuzzy C-mean – clusters (rules): [10 15 20 25 30]

Based on their studied range, the generalization performance and computational time are measured and illustrated in Fig. 11. In general, the computational time has a positive correlation with the number of tuning parameters. The less the number of tuning parameters, the less the computational time. However, the relationship between the generalization performance of the three fuzzy space partition methods and the number of tuning parameters is non-linear. The both trends of RSME obtained from grid partition and fuzzy C-mean methods can be observed from Fig. 11(a)(c) that are first a decrease and then an increase. More tuning parameters involved cannot improve generalization ability and consume a lot of computing resources.

In conjunction with Table 6 about best performance comparison of using three fuzzy space partition methods, fuzzy C-mean method has the lowest RMSE and affordable number of tuning parameters, compared to the other two. Although, sub. clustering method has the lowest computational time, the RMSE seriously increases 523% contrast to that obtained by fuzzy C-mean method. Therefore, Fuzzy C-mean methods with 20 rules setting is desirable solution for enhancing computational efficiency of the proposed GNFTL for in-cylinder pressure modelling.

4.4. Contribution on experimental reduction

In order to examine the contribution of the proposed GNFTL to the experimental reduction in practice, conventional manual design of experiment (DoE) is considered as a control group. Commonly, a skill technician as the main executor operates the entire experiment. According to the experimental routine introduced in Section 2.3, the fuel mass flow rate of biofuel will be measured to calculate the fuel consumption. Besides, operation time will also be estimated and considered in the comparison.

Table 5
results of four evaluation metrics of three designed segmentation patterns.

Segmentation	Evaluation metrics			
Pattern	MSE	RMSE	Error mean	Error St.D.
1D	44.69	6.68	1.25	6.57
2D	8.044	2.84	−0.25	2.83
Mixed	12.36	3.52	0.56	3.47

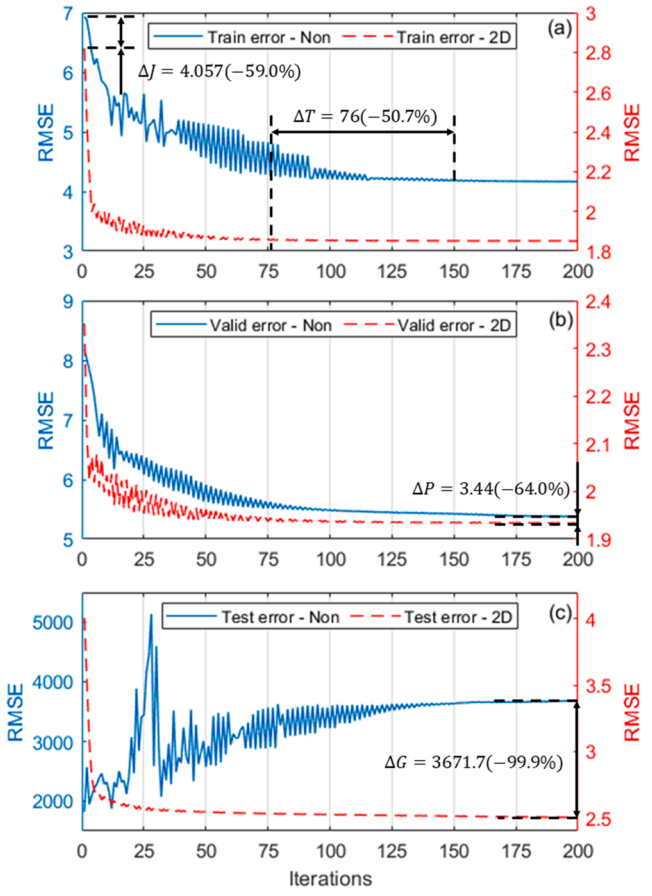

Fig. 8. Real-time performance comparison of non-transfer and transfer learning.

Table 7 collects experimental effort comparison of two experimental schemes, which includes diesel oil, MAO, operation time, and oil change time. The results are calculated based on a complete experimental routine with various testing conditions at 25, 50, 75, 100% power load, and 2000, 2400, 2800, 3200 rpm, and 0, 0.2, 0.5, 1 blending ratio of MAO. The manual DoE uses diesel oil of 6222 g and MAO of 4599 g to obtain experimental data used for in-cylinder pressure characterization. The GNFTL driven one uses diesel oil of 3641 g and MAO of 2691 g to obtain experimental data used for predictive modelling of in-cylinder pressure. Compared to the manual DoE, the GNFTL driven scheme can significantly reduce biofuel consumption by 47.8%, including diesel oil of 1623g and MAO of 950g. In terms of time cost during the entire experiment, the GNFTL driven scheme saves the time by 41.5%, contributed by testing time of 16 h. Fig. 12 depicts the perdition results of in-cylinder pressure with 75% power load and 1:1 MAO-diesel blends by using GNFTL-driven experimental scheme. As unsupervised domain data, this scheme still shows an excellent ability of function approximation with acceptable error mean (-0.25) and St.D. (2.83). By experimental validation, the proposed GNFTL illustrates that it has a great potential to save much experimental efforts in the research and

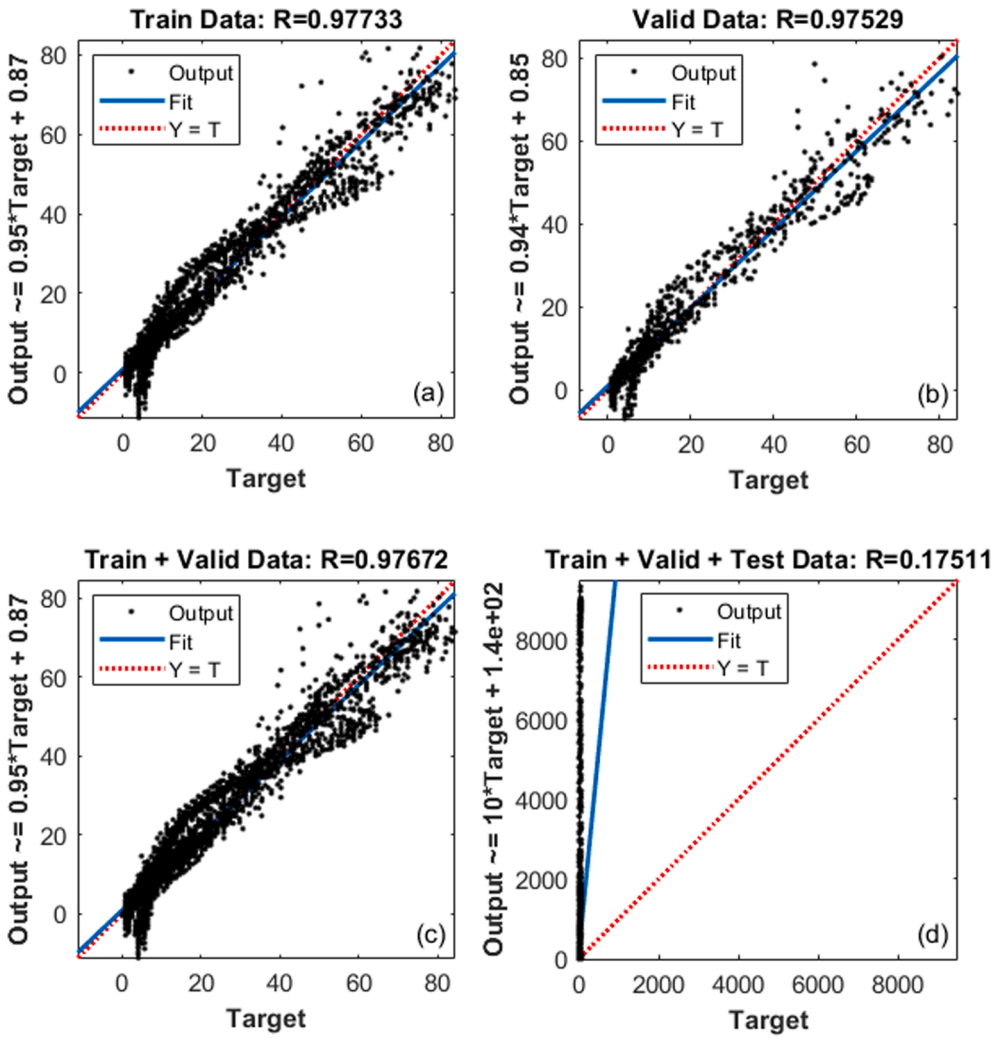

Fig. 9. Regression performance of using non-transfer learning.

development of biofuel and further speed up the pace to enter the market.

Table. 8 summarises the prediction performance of in-cylinder pressure with various blending ratios and power load conditions. In overall, the proposed approach demonstrates prediction accuracy with 3.71 bar (at 3200 rpm) to 5.22 bar (at 2800 rpm) of the peak pressure absolute error and 0.70 bar (at 3200 rpm) to 1.07 bar (at 2000 rpm) of absolute mean error. As the speed increases, absolute mean errors of in-cylinder pressure prediction gradually decreases, and finally drops to 0.7 bar at 3200 rpm. The authors think the reason behind this might be values of in-cylinder peak pressure at a high-speed condition of 3200 rpm is farther away from the boundary of its prediction interval (compared to other speed conditions). This makes it possible to avoid the discrepancy caused by exceeding the boundary or insufficient data in the transfer learning process. From a view of power load, the prediction accuracy at 50% and 75% power load are similar (Mean: 1.07 bar and 1.05 bar) but lower than those at 25% and 100% power load (Mean: 0.86 bar and 0.87 bar).

In terms of the generalization ability of the proposed approach, it has great potential to be applied to other engine parameters, different engine configurations, and biofuels with various physicochemical characteristics e.g. brake thermal efficiency and emissions. The main challenge for implementing this approach for various cases is to find the most effective features for such machine learning prediction systems. This would be the focus of our recent research.

5. Conclusions

This paper proposes a novel approach of geometric neuro-fuzzy transfer learning for in-cylinder pressure modelling of a diesel engine fuelled with MAO. Inspired by computational geometry, this approach only utilizes limited experimental data obtained by geometric screening to learn a high-precise transfer model of the in-cylinder pressure with different MAO-diesel blends. This is the first application of transfer learning in the field of internal combustion engines. An extensive numerical study of the proposed approach is carried out in terms of 1) impact of segmentation patterns; 2) transfer learning vs non-transfer learning; 3) fuzzy space partition methods; and 4) contribution on experimental reduction. The conclusions drawn from the investigation are as follows:

1) In three designed segmentation patterns for transfer domain of the engine operation region, using 2D segmentation pattern can significantly reduce the RMSE of 57.5% and 19.3%, respectively, compared to 1D and mixed them.
2) Compared to non-transfer learning applied in the in-cylinder pressure modelling, transfer learning performs excellent generalization performance that can effectively reduce initial error (before learning) by $\Delta J = 4.057(-59.0\%)$ and time to converge by $\Delta T = 76(-50.7\%)$.
3) In the comparison of fuzzy space partition method, desirable solution, fuzzy C-mean with 20 rules (260 tuning parameters) setting, is

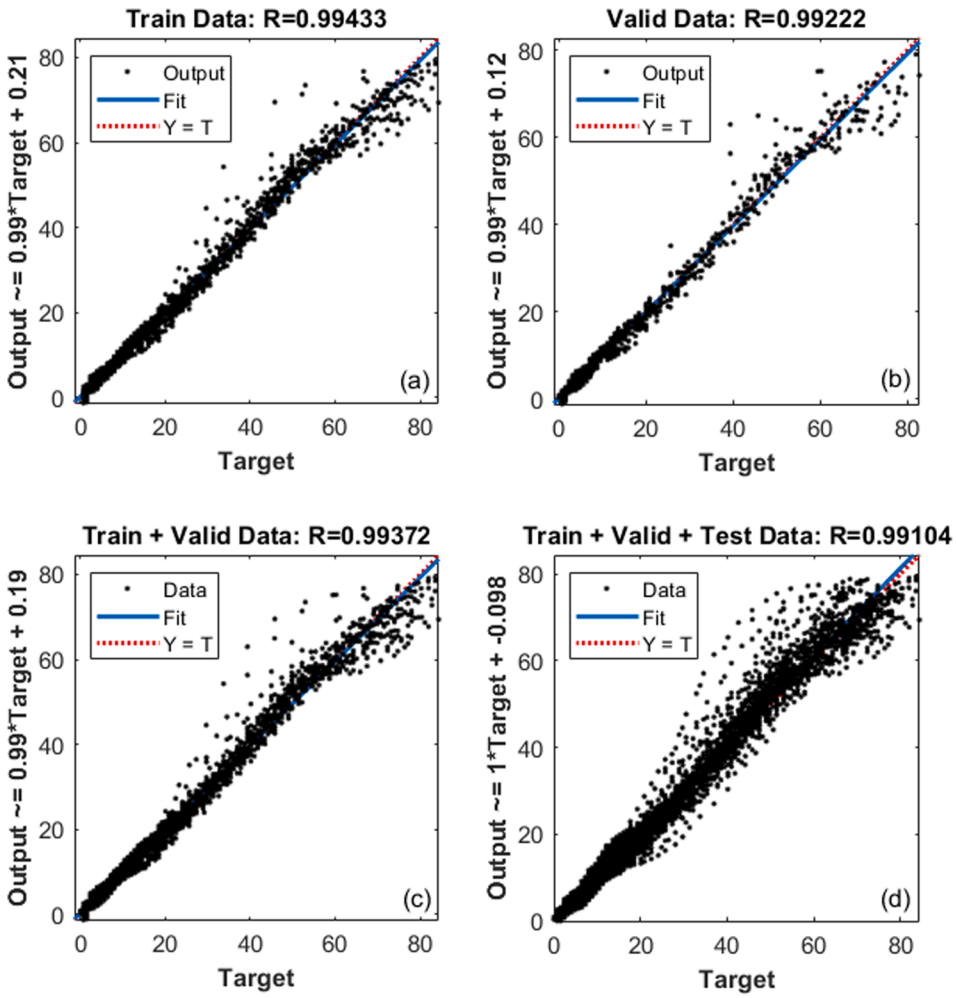

Fig. 10. Regression performance of using transfer learning.

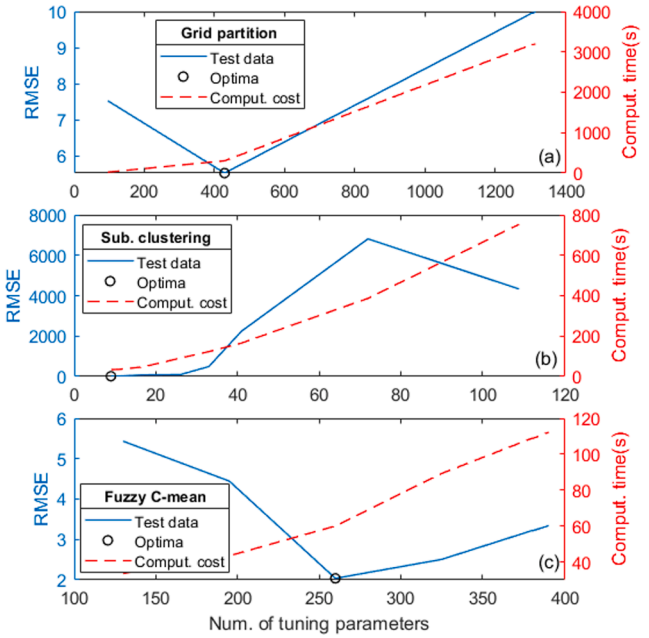

Fig. 11. The generalization performance and computational time comparison of three fuzzy space partition methods including: a) grid partition; b) sub. clustering; and c) fuzzy C-mean.

Table 6
Best performance comparison of using three fuzzy space partition methods.

Fuzzy space partition methods	RMSE	R^2	Num. of Rules	Num. of tuning parameters	Computational time (s)
Grid partition	5.533	0.9645	81	429	304
Sub. clustering	12.698	0.7873	9	117	34
Fuzzy C-mean	2.037	0.9952	20	260	60

found to enhancing computational efficiency of the proposed geometric neuro-fuzzy transfer learning.

4) The manual DoE uses diesel oil of 6222 g and MAO of 4599 g to obtain experimental data used for in-cylinder pressure characterization. The GNFTL driven one uses diesel oil of 3641 g and MAO of 2691 g to obtain experimental data used for predictive modelling of in-cylinder pressure. Compared to conventional manual DoE, the proposed approach can achieve a competitive prediction accuracy whilst significantly reducing biofuel consumption by 47.8% and operation time by 41.5%.

CRediT authorship contribution statement

Ji Li: Conceptualization, Methodology, Software, Writing – original draft. **Dawei Wu:** Conceptualization, Resources, Writing – review &

Table 7
Experimental effort comparison of two experimental schemes.

Experimental effort	Experimental scheme		Total reduction (%)
	Manual DoE	GNFTL driven	
Diesel oil (g)	6222	3641	47.8%
MAO (g)	4599	2691	
Testing time (hrs)	32	16	41.5%
Oil change time (hrs)	1.5	1.5	

editing, Funding acquisition. **Hassan Mohammadsami Attar:** Investigation, Data curation. **Hongming Xu:** Supervision, Writing – review & editing.

Declaration of Competing Interest

The authors declare that they have no known competing financial interests or personal relationships that could have appeared to influence the work reported in this paper.

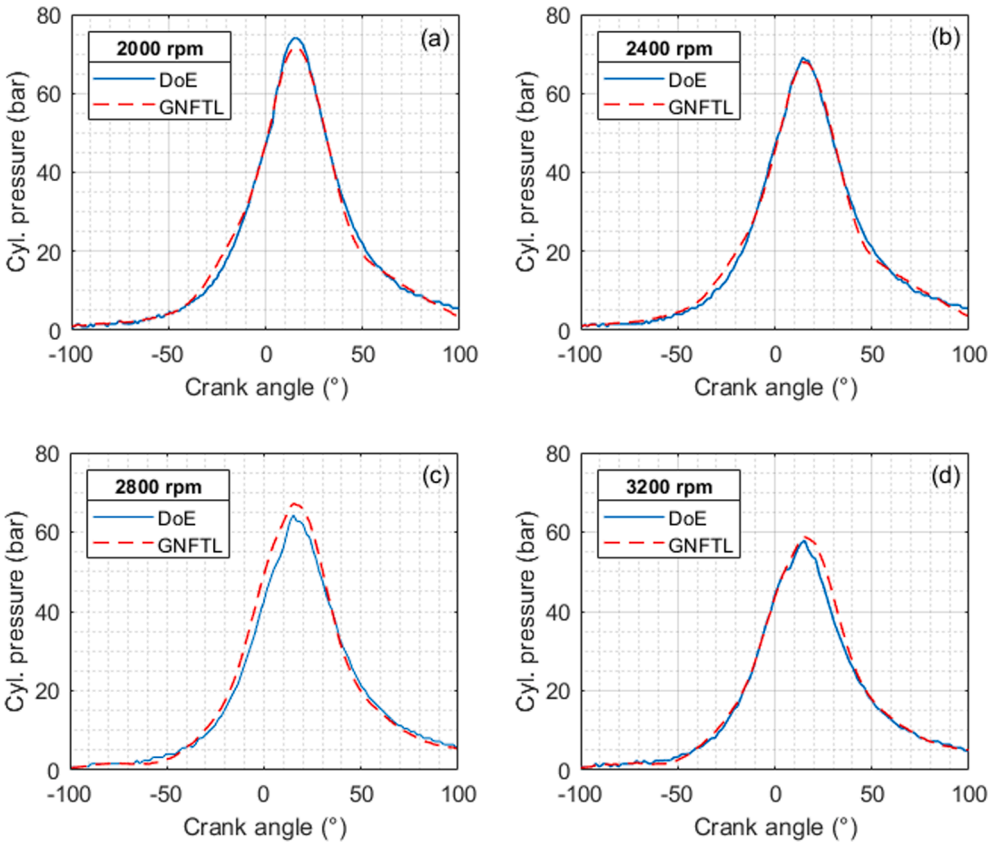

Fig. 12. Comparison of in-cylinder pressure with 75% power load and 1:1 MAO-diesel blends: a) at 2000 rpm; b) at 2400 rpm; c) at 2800 rpm; and d) at 3200 rpm.

Table 8
Comparison of in-cylinder pressure with various blending ratio and power load conditions.

Blending	Power	2000 rpm		2400 rpm		2800 rpm		3200 rpm	
Ratio	Load	Max (bar)	Mean (bar)	Max (bar)	Mean (bar)	Max (bar)	Mean (bar)	Max (bar)	Mean (bar)
	25%	4.41	1.04	5.32	0.89	5.23	0.87	4.79	0.86
0	50%	5.37	1.19	4.00	0.93	7.15	1.25	3.54	0.74
	75%	6.59	1.09	4.78	0.88	5.19	1.05	4.91	0.73
	100%	4.13	0.85	4.34	0.81	3.41	0.78	4.65	0.67
	25%	5.46	0.98	5.29	1.18	4.62	0.68	2.41	0.58
0.2	50%	5.26	1.06	3.68	0.96	6.23	1.24	3.97	1.08
	75%	5.33	1.21	2.28	0.82	7.70	1.53	3.86	0.93
	100%	5.04	1.04	4.64	0.98	6.14	1.14	3.18	0.47
	25%	3.41	0.88	4.14	1.06	4.63	0.71	2.09	0.52
0.5	50%	3.47	1.03	3.42	1.10	6.30	1.51	5.01	1.05
	75%	3.47	0.99	3.35	0.99	5.90	1.81	5.11	0.93
	100%	2.30	0.70	4.42	1.15	6.29	1.41	1.76	0.49
	25%	4.98	1.17	4.33	1.10	3.19	0.58	3.21	0.60
1	50%	4.98	1.42	7.03	1.27	3.85	0.69	2.96	0.55
	75%	5.57	1.24	5.85	1.45	4.19	0.68	3.05	0.50
	100%	5.28	1.25	4.30	1.11	3.51	0.61	4.79	0.52
Overall		4.69	1.07	4.45	1.04	5.22	1.03	3.71	0.70

Note: the indicators Max and Mean stand for in-cylinder peak pressure absolute error, and absolute mean error.

Acknowledgement

The authors appreciate the UK Engineering and Physical Sciences Research Council (EPSRC) for the financial support through the research grants EP/S00193X/1 and EP/S00193X/2.

References

[1] Reitz RD, Ogawa H, Payri R, Fansler T, Kokjohn S, Moriyoshi Y, et al. IJER editorial: The future of the internal combustion engine. Int J Engine Res 2020;21:3–10. https://doi.org/10.1177/1468087419877990.
[2] Raheem A, Prinsen P, Vuppaladadiyam AK, Zhao M, Luque R. A review on sustainable microalgae based biofuel and bioenergy production: Recent developments. J Clean Prod 2018;181:42–59. https://doi.org/10.1016/j.jclepro.2018.01.125.
[3] Yin Z, Zhu L, Li S, Hu T, Chu R, Mo F, et al. A comprehensive review on cultivation and harvesting of microalgae for biodiesel production: Environmental pollution control and future directions. Bioresour Technol 2020;301:122804. https://doi.org/10.1016/j.biortech.2020.122804.
[4] Lakshmikandan M, Murugesan AG, Wang S, Abomohra AEF, Jovita PA, Kiruthiga S. Sustainable biomass production under CO2 conditions and effective wet microalgae lipid extraction for biodiesel production. J Clean Prod 2020;247:119398. https://doi.org/10.1016/j.jclepro.2019.119398.
[5] Ramachandra TV, Durga Madhab M, Shilpi S, Joshi NV. Algal biofuel from urban wastewater in India: Scope and challenges. Renew Sustain Energy Rev 2013;21:767–77. https://doi.org/10.1016/j.rser.2012.12.029.
[6] Brennan L, Owende P. Biofuels from microalgae-A review of technologies for production, processing, and extractions of biofuels and co-products. Renew Sustain Energy Rev 2010;14:557–77. https://doi.org/10.1016/j.rser.2009.10.009.
[7] Singh A, Nigam PS, Murphy JD. Renewable fuels from algae: An answer to debatable land based fuels. Bioresour Technol 2011;102:10–6. https://doi.org/10.1016/j.biortech.2010.06.032.
[8] Yusri IM, Abdul Majeed APP, Mamat R, Ghazali MF, Awad OI, Azmi WH. A review on the application of response surface method and artificial neural network in engine performance and exhaust emissions characteristics in alternative fuel. Renew Sustain Energy Rev 2018;90:665–86. https://doi.org/10.1016/j.rser.2018.03.095.
[9] Shu J, Fu J, Zhao D, Liu J, Ma Y, Deng B, et al. Numerical investigation on the effects of valve timing on in-cylinder flow, combustion and emission performance of a diesel ignition natural gas engine through computational fluid dynamics. Energy Convers Manag 2019;198:111786. https://doi.org/10.1016/j.enconman.2019.111786.
[10] Otchere P, Pan J, Fan B, Chen W, Lu Y, Jianxing L. Mixture formation and combustion process of a biodiesel fueled direct injection rotary engine (DIRE) considering injection timing, spark timing and equivalence ratio – CFD study. Energy Convers Manag 2020;217:112948. https://doi.org/10.1016/j.enconman.2020.112948.
[11] Mahabadipour H, Srinivasan KK, Krishnan SR. An exergy analysis methodology for internal combustion engines using a multi-zone simulation of dual fuel low temperature combustion. Appl Energy 2019;256:113952. https://doi.org/10.1016/j.apenergy.2019.113952.
[12] Rakopoulos CD, Rakopoulos DC, Mavropoulos GC, Kosmadakis GM. Investigating the EGR rate and temperature impact on diesel engine combustion and emissions under various injection timings and loads by comprehensive two-zone modeling. Energy 2018;157:990–1014. https://doi.org/10.1016/j.energy.2018.05.178.
[13] Korsunovs A, Campean F, Pant G, Garcia-Afonso O, Tunc E. Evaluation of zero-dimensional stochastic reactor modelling for a Diesel engine application. Int J Engine Res 2020;21:592–609. https://doi.org/10.1177/1468087419845823.
[14] Tauzia X, Maiboom A, Karaky H. Semi-physical models to assess the influence of CI engine calibration parameters on NOx and soot emissions. Appl Energy 2017;208:1505–18. https://doi.org/10.1016/j.apenergy.2017.08.232.
[15] Nielsen KV, Blanke M, Eriksson L, Vejlgaard-Laursen M. Control-Oriented Model of Molar Scavenge Oxygen Fraction for Exhaust Recirculation in Large Diesel Engines. J Dyn Syst Meas Control Trans ASME 2017;139:1–10. https://doi.org/10.1115/1.4034750.
[16] Dong T, Liu B, Zhang F, Wang Y, Wang B, Liu P. Control oriented modeling and analysis of gas exchange and combustion processes for LTC diesel engine. Appl Therm Eng 2017;110:1305–14. https://doi.org/10.1016/j.applthermaleng.2016.09.001.
[17] Maroteaux F, Saad C, Aubertin F. Development and validation of double and single Wiebe function for multi-injection mode Diesel engine combustion modelling for hardware-in-the-loop applications. Energy Convers Manag 2015;105:630–41. https://doi.org/10.1016/j.enconman.2015.08.024.
[18] Wang L, Liu Z, Miao Q, Zhang X. Time–frequency analysis based on ensemble local mean decomposition and fast kurtogram for rotating machinery fault diagnosis. Mech Syst Signal Process 2018;103:60–75. https://doi.org/10.1016/j.ymssp.2017.09.042.
[19] Quérel C, Grondin O, Letellier C. Semi-physical mean-value NOx model for diesel engine control. Control Eng Pract 2015;40:27–44. https://doi.org/10.1016/j.conengprac.2015.02.005.
[20] Turkson RF, Yan F, Ali MKA, Hu J. Artificial neural network applications in the calibration of spark-ignition engines: An overview. Eng Sci Technol an Int J 2016;19:1346–59. https://doi.org/10.1016/j.jestch.2016.03.003.
[21] Raghuvaran S, Ashok B, Veluchamy B, Ganesh N. Evaluation of performance and exhaust emission of C.I diesel engine fuel with palm oil biodiesel using an artificial neural network. Mater Today Proc 2020;37:1107–11. https://doi.org/10.1016/j.matpr.2020.06.344.
[22] Hosseini SH, Taghizadeh-Alisaraei A, Ghobadian B, Abbaszadeh-Mayvan A. Artificial neural network modeling of performance, emission, and vibration of a CI engine using alumina nano-catalyst added to diesel-biodiesel blends. Renew Energy 2020;149:951–61. https://doi.org/10.1016/j.renene.2019.10.080.
[23] Dey S, Reang NM, Majumder A, Deb M, Das PK. A hybrid ANN-Fuzzy approach for optimization of engine operating parameters of a CI engine fueled with diesel-palm biodiesel-ethanol blend. Energy 2020;202:117813. https://doi.org/10.1016/j.energy.2020.117813.
[24] Kumar S. Estimation capabilities of biodiesel production from algae oil blend using adaptive neuro-fuzzy inference system (ANFIS). Energy Sources, Part A Recover Util Environ Eff 2020;42:909–17. https://doi.org/10.1080/15567036.2019.1602203.
[25] Singh NK, Singh Y, Sharma A, Rahim EA. Prediction of performance and emission parameters of Kusum biodiesel based diesel engine using neuro-fuzzy techniques combined with genetic algorithm. Fuel 2020;280:118629. https://doi.org/10.1016/j.fuel.2020.118629.
[26] Najafi B, Akbarian E, Lashkarpour SM, Aghbashlo M, Ghaziaskar HS, Tabatabaei M. Modeling of a dual fueled diesel engine operated by a novel fuel containing glycerol triacetate additive and biodiesel using artificial neural network tuned by genetic algorithm to reduce engine emissions. Energy 2019;168:1128–37. https://doi.org/10.1016/j.energy.2018.11.142.
[27] Fagundez JLS, Lanzanova TDM, Martins MES, Salau NPG. Joint use of artificial neural networks and particle swarm optimization to determine optimal performance of an ethanol SI engine operating with negative valve overlap strategy. Energy 2020;204:117892. https://doi.org/10.1016/j.energy.2020.117892.
[28] Uslu S. Optimization of diesel engine operating parameters fueled with palm oil-diesel blend: Comparative evaluation between response surface methodology (RSM) and artificial neural network (ANN). Fuel 2020;276:117990. https://doi.org/10.1016/j.fuel.2020.117990.
[29] Ye W, Wang X, Liu Y, Chen J. Analysis and prediction of the performance of free-piston Stirling engine using response surface methodology and artificial neural network. Appl Therm Eng 2021;188:116557. https://doi.org/10.1016/j.applthermaleng.2021.116557.
[30] Anenberg SC, Miller J, Minjares R, Du L, Henze DK, Lacey F, et al. Impacts and mitigation of excess diesel-related NO x emissions in 11 major vehicle markets. Nature 2017;545:467–71. https://doi.org/10.1038/nature22086.
[31] Joshi G, Pandey JK, Rana S, Rawat DS. Challenges and opportunities for the application of biofuel. Renew Sustain Energy Rev 2017;79:850–66. https://doi.org/10.1016/j.rser.2017.05.185.
[32] Gao Z, Deng Y, Wen Y, Lu J, Du Z, Tang C, et al. Deep-learning based in-cylinder pressure modeling and resolution of ion current signals. Fuel 2020;282:118722. https://doi.org/10.1016/j.fuel.2020.118722.
[33] Shrivastava N, Khan ZM. Application of Soft Computing in the Field of Internal Combustion Engines: A Review. Arch Comput Methods Eng 2018;25:707–26. https://doi.org/10.1007/s11831-017-9212-9.
[34] Li J, Li Z, Zhou Q, Zhang Y, Xu H. Improved scheme of membership function optimisation for fuzzy air-fuel ratio control of GDI engines. IET Intell Transp Syst 2018;13:209–17. https://doi.org/10.1049/iet-its.2018.5013.
[35] Pan SJ, Yang Q. A Survey on Transfer Learning. IEEE Trans Knowl Data Eng 2010;22. https://doi.org/10.1007/978-981-15-5971-6_83.
[36] Attar HM, Wu D, Harvey AP. Performance, Emissions and Durability Studies on Diesel Engine Fuelled with a Preheated Raw Microalgal Oil. Proceedings 2020;58:4. 10.3390/wef-06906.
[37] Li P, Sakuragi K, Makino H. Extraction techniques in sustainable biofuel production: A concise review. Fuel Process Technol 2019;193:295–303. https://doi.org/10.1016/j.fuproc.2019.05.009.
[38] Cocco Mariani V, Hennings Och S, dos Santos CL, Domingues E. Pressure prediction of a spark ignition single cylinder engine using optimized extreme learning machine models. Appl Energy 2019;249:204–21. https://doi.org/10.1016/j.apenergy.2019.04.126.
[39] Solmaz O, Gurbuz H, Karacor M. Comparison of artificial neural network and fuzzy logic approaches for the prediction of in-cylinder pressure in a spark ignition engine. J Dyn Syst Meas Control Trans ASME 2020;142:1–11. https://doi.org/10.1115/1.4047014.
[40] Zhuang F, Qi Z, Duan K, Xi D, Zhu Y, Zhu H, et al. A comprehensive survey on transfer learning. Proc IEEE 2020;109.
[41] Jang JR. ANFIS : Adaptive-Network-Based Fuzzy Inference System. IEEE Trans Syst Man: Cybern Syst; 1993. p. 23.
[42] Brown M, Harris CJ. Neurofuzzy adaptive modelling and control. Prentice Hall; 1993.
[43] Taylor ME, Stone P. Transfer Learning for Reinforcement Learning Domains: A Survey. J OfMachine Learn Res 2009;10:1633–85. https://doi.org/10.1007/978-3-642-27645-3_2.